Glass-ceramic scaffolds containing silica mesophases for bone grafting and drug delivery

Chiara Vitale-Brovarone, Francesco Baino, Marta Miola, Renato Mortera, Barbara Onida, Enrica Verné*

Materials Science and Chemical Engineering Department, Politecnico di Torino, Torino, Italy

*Corresponding author: Enrica Verné
Tel.: +39 011 5644717
Fax: + 39 011 5644699
E-mail address: enrica.verne@polito.it

Abstract

Glass-ceramic macroporous scaffolds were prepared using glass powders and polyethylene (PE) particles of two different sizes. The starting glass, named as Fa-GC, belongs to the system SiO_2-P_2O_5-CaO-MgO-Na_2O-K_2O-CaF_2 and was synthesized by a traditional melting-quenching route. The glass was ground and sieved to obtain powders of specific size which were mixed with PE particles and then uniaxially pressed in order to obtain crack-free green samples. The compact of powders underwent a thermal treatment to remove the organic phase and to sinter the Fa-GC powders. Fa-GC scaffolds were characterized by means of X-Ray Diffraction, morphological observations, density measurements, image analysis, mechanical tests and *in vitro* tests. Composite systems were then prepared combining the drug uptake-delivery properties of MCM-41 silica micro/nanospheres with the Fa-GC scaffold. The system was prepared by soaking the scaffold into the MCM-41 synthesis batch. The composite scaffolds were characterized by means of X-Ray Diffraction, morphological observations, mechanical tests and *in vitro* tests. Ibuprofen was used as model drug for the uptake and delivery analysis of the composite system. In comparison with the MCM-41-free scaffold, both the adsorption capacity and the drug delivery behaviour were deeply affected by the presence of MCM-41 spheres inside the scaffold.

Keywords: *composite; glass-ceramic scaffold; bone grafting; MCM-41; drug delivery*

1 Introduction

Bone tissue engineering aims to the reconstruction or substitution of human bone where bone loss, due to trauma, tumours, osteoporosis, periodontal resorption or arthroplasty revision occurred [1,2,3]. Bone regeneration using autografts is the most advantageous technique because eliminates problems of immune rejection and pathogen transfer. Nevertheless, the limited bone availability, the risk of donor site morbidity and of chronic pain in the explantation site make this method sometimes unsuitable [4]. For what concerns the use of allografts, these implants involve the potential immune rejection and the transmission of pathogen diseases [5]. Due to the drawbacks of autografts/allografts implants, tissue engineering represents an alternative approach to repair the damaged tissues using synthetic

biomaterials to produce scaffolds [6]. In fact alloplastic materials, being synthetic, overcome antigenity and morbidity issues and can be available in unlimited amounts. Among ceramic materials for bone scaffolding, hydroxyapatite (HAp), β-tricalcium phosphate (β-TCP) and bioactive glasses and glass-ceramics have been widely investigated [7,8]. 3D glass and glass-ceramic scaffolds ought to exhibit a highly porous, open structure in order to promote an effective vascularisation of the implant and should possess a mechanical strength comparable with cancellous bone (2-12 MPa) [9]. Besides, it is reported that a good osteointegration can be attained with a macroporous interconnected network, with pores size within 100-600 μm [10]. Microporosity is also important because favours protein adhesion and thus cells attachment on the scaffold and allows the flow of nutrient to cells within the scaffold [11]. The scaffold ability in stimulating bone regeneration is well known in literature as bioactivity, *i.e.* a complex mechanism of ion exchange that leads to the precipitation of a HAp layer on the scaffold surface during the contact with body fluids. The HAp layer promotes an effective osteointegration of the implant by creating a strong chemical bond with the surrounding bone tissue [12-14]. Different methods can be used to prepare glass and glass-ceramic scaffolds for tissue engineering, for example starch consolidation, sponge replication, direct foaming and freeform fabrication techniques [15-20]. Specifically, in this work polyethylene particles were used as pore-former agents and the macroporous scaffolds were obtained through the burning out of the organic phase and the sintering of the glass powders.

After a biomaterial implantation, a serious problem that might occur is the adverse inflammatory response of the body with the related complications, such as septicaemia [21,22]. For this reason, anti-inflammatory drugs and antibiotics are

given to the patient with a consequent increase of the healing time. For this reason, the development of systems coupling bone regeneration and drug delivery ability is a promising field of applied research. In fact, an implantable system able to deliver drug molecules presents a lot of advantages, such as the reduction of the total drug dosage introduced in the body, a precise drug setting in the implant zone and the tuning of the drug release kinetics.

In the last years, ordered mesoporous materials came out as candidates for drug delivery applications and since their discovery in 1992, the ordered mesoporous silica attracted the interest of many scientists [23]. Mesoporous systems possess a highly ordered mesoporous structure which can be tuned by changing the synthesis conditions, and can be prepared in different forms, such as thin films, monoliths or powders. One of the most interesting research field is the employment of mesoporous systems as host matrices for functional molecules, such as enzymes, dyes or drugs [24-26].

In a previous work [26], SBA-15 mesoporous silica were incorporated inside a bioactive glass-ceramic scaffold belonging to the SiO_2-CaO-K_2O system (SCK) and produced through the burning-out method [27] in order to obtain a composite scaffold able to promote the successful integration of the graft and the local drug delivery in the implant zone. This composite system showed a drawback related to the SBA-15 synthesis conditions (strongly acidic) which lead to the SCK scaffold degradation during the mesophase loading. In a following work [28], the study was extended to MCM-41 silica spheres, that posses narrower pores size in comparison with SBA-15, and the synthesis conditions were optimised in order to avoid the scaffold damage (pH about 9).

This research work is focused on the preparation and characterization of an implantable composite system, formed by a glass-ceramic scaffold of complex

composition, containing fluoroapatite crystals, and MCM-41, in whose nanopores the drug was incorporated. At this purpose the scaffolds were used as carriers for MCM-41 micro/nanospheres and the composite system was loaded with the drug molecules. The procedure followed to prepare MCM-41 [29] allows obtaining sub-micronic spherical particles, with nanopores average size about 2 nm. The model drug chosen for the up-take and delivery studies was ibuprofen, widely adopted in literature [24,30-31].

2 Experimental

A glass-ceramic containing fluoroapatite crystals with the following molar composition, 50% SiO_2, 18% CaO, 9% CaF_2, 7% Na_2O, 7% K_2O, 6% P_2O_5, 3% MgO (Fa-GC) [32], was chosen to prepare the scaffolds.

Fa-GC was produced by melting the raw products (SiO_2, $Ca_2P_2O_7$, $CaCO_3$, $(MgCO_3)_4{\cdot}Mg(OH)_2{\cdot}5H_2O$, Na_2CO_3, K_2CO_3, CaF_2) in a platinum crucible at 1550°C for 1 hour and by quenching the melt in water to obtain a frit that was subsequently ball milled and sieved to a final grain size below 106 μm. X-Ray diffraction (X'Pert Philips diffractometer) using the Bragg Brentano camera geometry and the Cu-Kα incident radiation were carried out on as quenched Fa-GC powders; the pattern analysis was carried out using X'Pert High Score software and the PCPDF data bank. The pattern of as poured Fa-GC showed the existence of an amorphous halo and of many diffraction peaks identified as fluoroapatite (PCPDF reference code 01-076-0558).

The values of T_g (glass transition temperature), T_X (crystallization temperature) and T_l (liquidus temperature) were assessed using differential thermal analysis (DTA7 Perkin-Elmer) with an heating rate of 20 °C/min from 50 to 1500 °C.

In order to select the heat treatment conditions for the scaffold production, hot stage microscopy was carried out; at this purpose, a 3 mm × 3 mm × 3 mm "green" of Fa-GC powders was progressively heated up to 1100 °C and its dimensional variations were monitored through a web-cam while increasing temperature.

2.1 Scaffolds preparation

The scaffolds were prepared by mixing Fa-GC powders, sieved below 106 μm, with a thermally removable organic phase acting as pore former. For this purpose, two different polyethylene particles were used in order to introduce macropores of different sizes.

The used polyethylene powders are listed below:

PE1: particles size within 90-150 μm;

PE3: particles size within 300-600 μm.

Fa-GC powders sieved below 106 μm and polyethylene particles were carefully mixed together for 30′ in a plastic bottle using a roll shaker to obtain an effective mixing. In this research, various amounts of polyethylene were added to Fa-GC powders in order to produce different series of scaffolds. In particular, the polyethylene amount was varied within 40% to 70% vol. to evaluate the best compromise between high porosity content and satisfactory mechanical strength.

The scaffolds will be named, from now on, with an acronym indicating the type and the amount of used polyethylene particles; for instance PE1-70 indicates the series of scaffolds obtained using 70% vol. of PE1 particles.

Compacts of powders ("greens") were obtained through uniaxial pressing of the mixed powders without the addition of any binder. The applied pressure and time were optimised in order to obtain crack free greens: the best conditions were identified with a pressure of 127 MPa for 10 s. The greens were shaped in form of disks (3 cm of diameter, 0.5 cm of thickness) for the morphological and *in vitro* characterization and in form of bars (5 cm × 1 cm × 1 cm) for the mechanical tests. The green bodies were then introduced into a furnace at room temperature and thermally treated in air aiming to remove the polyethylene powders and to sinter the inorganic phase obtaining macroporous glass-ceramic scaffolds. The thermal treatment was set at a final temperature of 800 °C for 3 hours, with a heating and cooling rate of 10 °C/min, and was chosen on the basis of hot stage microscopy and DTA studies carried out on Fa-GC powders. Finally, the sintered bars were cut with a low speed diamond saw to obtain 1 cm × 1 cm × 1 cm macroporous scaffolds.

2.2 Synthesis of MCM-41 spheres on Fa-GC scaffolds

PE1-70 and PE3-50 exhibited the finest compromise between degree of porosity and mechanical strength for the PE1 and PE3 scaffolds series and were then used as carriers for MCM-41 micro/nanospheres loaded with ibuprofen (herein named MCM-41-PE1-70 and MCM-41-PE3-50). Mesoporous MCM-41 nanospheres were synthesised and precipitated directly inside the scaffolds in order to obtain a composite material. The MCM-41 synthesis solution was prepared modifying, as previously reported [28], a standard recipe [29], using n-hexadecyltrimethylammonium bromide (C_{16}TMABr) as surfactant template. Reactant molar ratio was: 1 TEOS : 0,3 C_{16}TMABr : 0,129 NH_3 : 144 H_2O : 58

EtOH. The surfactant (C_{16}TMABr) was dissolved into the mixture of distilled water, NH_3 and EtOH; tetraethylorthosilicate ($[C_2H_5O]_4Si$, TEOS) was then added to the surfactant solution under continuous stirring for 10′. After this time, the cubic scaffold was soaked for 12′ directly in the solution at pH about 9. In this way, the MCM-41 nanospheres precipitated onto the scaffold and inside its macropores. After the MCM-41 precipitation, the impregnated scaffold were aged at 90 °C for 24 h in air, and then calcined through a two steps process (1 h at 200 °C in nitrogen, 7 h at 450 °C in air). The proposed ageing treatment, besides allowing the complete formation and growing of MCM-41 spheres, may also promote the formation of Si—O—Si bridges between the scaffold and the mesophase. The calcination eliminates the surfactant and consolidates the ordered mesoporous structure. In such a way a composite scaffold containing MCM-41 micro/nanospheres was successfully obtained.

2.3 As-done and composite scaffolds characterization

The morphology of the scaffolds was studied through scanning electron microscopy (SEM, Philips 525 M) in order to observe the degree of sintering (presence of dense sintering necks) and to evaluate the morphology and distribution of the pores. In particular, cross-sections of the scaffolds were observed to evaluate the homogeneity of pores distribution along the section, the degree of their interconnection and the influence of the type and amount of used polyethylene particles (PE1, PE3).

The total pores content (% vol.) was evaluated by density measurements carried out by using the formula $\left(1-\frac{W_m}{W_{th}}\right)\times 100$, where W_m is the measured weight and W_{th} the theoretical one extracted from the product of glass density and the sample volume.

For this purpose, 10 samples of each scaffold series were weighed and measured.

To guarantee an effective cells migration inside the whole scaffold, the pores size and degree of interconnection is a crucial aspect and for this reason the porosity was further investigated on different scaffold cross-sections through image analysis (software Qwin Leica). This technique is practical to assess the pore size distribution and the total pore amount; it uses different SEM micrographs on which a measurement window is selected and the porosity is highlighted by increasing the black and white contrast. Afterwards, the software elaborates the image as a binary picture identifying the dark areas as pores: the equivalent pore diameter is then evaluated as $2\sqrt{A/\pi}$, where A is the effective area calculated by the software. The acquired data can be further processed in order to plot them as bar charts reporting the pores numbers or the pores area versus the pores equivalent diameter.

Mercury porosimetry was not adopted to analyse the samples because this technique allows to detect only pores below 100 μm, whereas for bone scaffolds a key role is played by macropores which should be open and interconnected.

The strength of the scaffolds was evaluated through destructive compressive tests on 1 cm × 1 cm × 1 cm cubic samples using an Instron machine at 1.0 mm/min of crosshead speed and testing 5 different specimens obtained from the same bar.

The porous samples were tested in the three spatial directions to put into evidence possible anisotropy of the scaffold. The compressive strength was obtained dividing the maximum load registered during the test by the resistant section area.

The mechanical characterization was carried out both on the as done scaffolds and on the composite scaffolds in order to verify eventual mechanical damages due to the MCM-41 particles loading.

The presence of MCM-41 inside the scaffolds was assessed by means of XRD analysis at low angles (2-10°). Then MCM-41 loading onto the scaffold was investigated through SEM observation on the scaffold surface and on different cross-sections in order to observe the penetration depth of MCM-41 spheres through the scaffold porosity.

The study of the *in vitro* bioactivity was performed by soaking the as done scaffolds and the composite ones in a simulated body fluid (SBF) [33] for different times up to 1 month. Specifically the samples (1 cm × 1 cm × 1 cm) were soaked in 30 ml of SBF, maintained at 37 °C in polyethylene bottles with a refresh of the solution every 48 h to simulate the flow of physiological fluids.

2.4 Ibuprofen uptake and delivery

The drug loading ability of the composite scaffolds was tested on the MCM-41-PE1-70 series of scaffolds. At this aim, at room temperature, 9 ml of ibuprofen in pentane solution (33 mg/ml, 0.160 M) was put into contact with the composite MCM-41- PE1-70 scaffold for 72 h without stirring. The drug uptake was evaluated through UV-visible spectrophotometry (Cary 500 Scan, wavelength λ = 263 nm, molar extinction coefficient ε_λ = 320 $M^{-1}cm^{-1}$) and was assessed in terms of ibuprofen concentration variation in the solution before and after the scaffold soaking. The drug release kinetics were evaluated *in vitro* by soaking the composite scaffolds in 30 ml of stirred SBF maintained at 37 °C [28]. At different time frames, a small amount of SBF (1 ml) was picked-up and analysed through UV-visible spectrophotometry (λ = 263 nm, ε_λ = 440 $M^{-1}cm^{-1}$) to assess the amount of released ibuprofen.

3 Results

3.1 Fa-GC

Figure 1 reports the DTA trace of as quenched Fa-GC powders: the exothermal peaks at 730 °C and 780 °C were attributed to the nucleation of two crystalline phases.

XRD pattern on as melt Fa-GC powders is reported in fig. 2a whereas the diffraction pattern obtained for the scaffold after the thermal treatment is shown in fig. 2b. As it can be observed, as-poured Fa-GC is a glass-ceramic containing fluoroapatite crystals (PCPDF reference code 01-076-0558) and the thermal treatment, carried out to produce the scaffolds, induced the crystallisation of the residual amorphous phases and the nucleation of a new crystalline phase that was identified as canasite (JCDD 00-013-0553). The DTA analysis carried out on the as poured Fa-GC showed the presence of two exothermic peaks signifying that from the residual glassy phase the crystallisation of fluoroapatite continues.

The modification of the sample area observed during hot stage microscopy is reported in figure 3. Fa-GC shows an expansion at about 550 °C due to thermal expansion and a shrinkage beginning just below 600 °C. The maximum shrinkage was observed at 700 °C and after it, owing to crystallization phenomena, the sample slightly expands according to DTA results (fig. 1).

3.2 Fa-GC scaffolds

PE1-series scaffolds were successfully obtained using polyethylene (PE) amounts ranging within 40% vol. and 70% vol. At this purpose, figure 4a reports a PE1-40

cross-section: the pores are open and in the range of 100-200 μm with very dense sintering necks.

Due to the good sintering degree observed for PE1-40, the organic content was augmented till 70 % vol. in order to increase the total porosity; figure 4b reports the cross-section of PE1-70 and figure 4c a pore magnification in which the glass-ceramic nature of the scaffold and the pore interconnection can be observed.

Generally, by increasing the PE content the pores amount increases but also gradually the scaffold mechanical strength decreases. Therefore, it is crucial to identify the maximum PE content allowing satisfactory mechanical properties and a good degree of sintering. Besides, the influence of MCM-41 synthesis on the scaffold integrity should be considered, as in a previous work it negatively affected the integrity of the scaffold [26].

PE particles ranging within 300-600 μm were used to prepare the PE3-series scaffolds which are characterized by larger macropores. At this purpose, figure 5a reports a micrograph of a polished PE3-50 cross-section where pores as large as 100-500 μm can be seen. Figure 5b shows the interconnection of the pores and figure 5c depicts the very good sintering degree of Fa-GC powders and the glass-ceramic nature of the obtained scaffolds.

Table 1 reports the porosity values for PE1-70 and PE3-50, *i.e.* the samples that will be loaded with MCM-41 in the second part of the work; density measurements were carried out on 10 specimens for each series.

The introduced porosity was further investigated through image analysis on polished sections of the scaffold using the Qwin Program of Leica as described in subsection 2.3.

Figure 6a reports, as an example, a micrograph of a PE1-70 section and figure 6b the processed image in which the darker areas are pores that will be identified by

the program as empty spaces. Figure 7 depicts in a bar chart the results of the image analysis carried out on both PE1-70 and PE3-50. The presence of both micropores (below 100 μm) and macropores (100-600 μm) can be observed, but the amount of the formers is widely prevailing on the latter ones (figure 7a). In figure 7b the porosity was calculated considering the total area occupied by pores having a specific size range and expressed as a percentage of the whole area taken by the pores.

3.3 MCM-41-PE1-70 and MCM-41-PE3-50 composites

The success of the incorporation of MCM-41 inside the scaffold was investigated through low-angle XRD analysis and SEM characterization.

XRD analysis was performed on both calcined and non-calcined samples.

In figure 8 patterns of MCM-41-PE1-70 before (pattern 1) and after the calcination (pattern 2) are compared. Both graphs show the peak due to the (100) reflection, whereas no peaks due to (110) and (200) reflections are observed. A similar pattern is observed for MCM-41 powders prepared in similar conditions [28] (inset in the figure pattern A). The lack of defined (110) and (200) peaks is ascribed to a low degree of the hexagonal mesoscopic order, due to the lower alkalinity used in the synthesis (pH about 9) with respect to typical MCM-41 synthesis procedure (pH about 11) [29]. In fact it is known that lower alkalinity usually favours the formation of disordered phases [34].

After calcination an increase in (100) peak intensity is observed, due to the elimination of surfactant micelles inside mesopores, as usually observed for MCM-41 powders. A small decrease of d_{100} value also occurs from 3.42 nm to 3.39 nm, due to the shrinkage of the structure upon calcination.

Figure 9a shows the MCM-41-PE1-70: a large amount of MCM-41 agglomerates all over the scaffold surface can be observed.

Figure 9b reports the detail of an interconnected double pore with a dense trabecula on which the white agglomerates of MCM-41 particles can be seen.

Figure 10a shows the magnification of a macropore (diameter about 250 μm) in which the good anchorage of MCM-41 spheres can be observed. Figure 10b reports an enlargement of an agglomerate of MCM-41 spheres: as it can be observed the spheres are of sub-micronical size (within 100 nm-1 μm).

The penetration depth of MCM-41 spheres inside the scaffold was investigated through SEM observation on the composite scaffold cross-sections and the maximum MCM-41 infiltration profundity was about 1 mm.

Figure 11 shows MCM-41 spheres agglomerates on PE3-50 surface; similar agglomerates were observed on PE3-50 cross-section.

As far as the penetration depth of mesophase inside MCM-41-PE3-50 scaffolds is concerned, a better penetration was observed (about 2 mm) in comparison with MCM-41-PE1-70.

3.4 Mechanical strength tests

Fa-GC scaffolds of PE1-70 and PE3-50 series and composite scaffolds (MCM-41-PE1-70 and MCM-41-PE3-50) were tested in compression using 1 cm × 1 cm × 1 cm cubic samples; the obtained results are reported in table 2. The obtained values are comparable with the mechanical strength of human bone [9].

The PE1-70 showed higher values compared to PE3-50, due to the presence of smaller pores: in fact an increase in the pores size generally involves a decrease in the compressive strength.

The composite scaffolds (MCM-41-PE1-70 and MCM-41-PE3-50), tested under the same conditions, exhibited values of compressive strength analogous to MCM-41-free scaffolds.

3.5 In vitro bioactivity

The *in vitro* bioactivity of both as-done scaffolds and of MCM-41-loaded ones was assessed through soaking them in SBF for 1 week and 1 month. All the tested samples belonged to PE1-70 series. Figure 12 shows HAp agglomerates observed on the scaffold surface after 1 week in SBF. The variations of pH values in SBF, induced by ion release, were measured twice a week during the bioactivity tests: the maximum pH value was 7.55.

No significant differences were observed between MCM-41-loaded scaffolds and as-done scaffolds during the bioactivity tests.

3.6 Ibuprofen uptake and delivery

The aims of this study can be summarized as listed below:

i) to investigate if MCM-41-PE1-70 composite absorbs a greater amount of ibuprofen in comparison with non-loaded scaffolds;

ii) to investigate if MCM-41 inside Fa-GC scaffold plays a role in ibuprofen molecules release, in view of controlled drug delivery.

For these purposes, a Fa-GC scaffold, used as reference (herein denoted as PE1-70-ref), has been soaked in the MCM-41 synthesis solution without TEOS.

The analysis time for ibuprofen up-take is 72 h. As it can be observed in table 3, the amount of ibuprofen absorbed by MCM-41-PE1-70 is about 10 times greater than the PE1-70-ref one.

The analysis time for ibuprofen release was 96 h. As it can be observed in figure 13, MCM-41-PE1-70 delivers a greater amount of drug in comparison with PE1-70-ref because the latter one, during the uptake, absorbed a smaller ibuprofen amount; these results are consistent with uptake ones.

The release curve resembles that observed for MCM-41 powder and other MCM-41 containing scaffold [28, 35-36], confirming that ibuprofen delivery does occur from the mesoporous phase.

4 Discussion

In this work, 3D glass-ceramic scaffolds were prepared via uniaxial pressing of a mixture composed by Fa-GC powders and PE particles as pore formers. The scaffolds were obtained through a thermal treatment in order to remove the organic phase and to sinter the inorganic one.

The thermal treatment is a crucial step for the scaffolds preparation, as a satisfactory degree of sintering must be achieved without structure collapse due to PE pyrolysis. The temperature for the thermal treatment was chosen on the basis of Fa-GC hot stage microscopy results, which shows that the maximum shrinkage of Fa-GC occurs at 700 °C (fig. 3). Due to the DTA results which showed T_{XX} below 800°C, this temperature was set as the sintering one in order to benefit from a good shrinkage of Fa-GC and of its crystallisation into fluorapatite and canasite which are known to be highly biocompatible and osteconductive phases. The green samples were introduced at room temperature into the furnace and thermally

treated at 800 °C for 3 h. The TGA trace of PE showed the complete removal of the organic phase at 500 °C, thus no contamination of the Fa-GC scaffolds is foreseen after sintering and was actually found.

The obtained scaffolds are characterized by open and interconnected macropores; for instance figures 4a, 4c and 5b show the presence of interconnected macropores, which is a very important feature as a high degree of interconnection is crucial to attain a fast viability of the inner parts of the scaffold and to promote an effective bone in-growth *in vivo*.

The SEM investigations showed that a high degree of sintering was achieved as it is possible to see in fig. 4 and 5. The trabeculae are characterized by a dispersed microporosity as it can be observed in fig. 4b and 5b, which is known to be useful for cell adhesion *in vivo* [11], and in the present work may also help the anchorage of MCM-41 spheres. Besides, the presence of micropores is essential for the flow of nutrients and waste products inside the scaffold in order to allow a proper environment for cells in the whole structure. The scaffold roughness (fig. 5c) due to the presence of crystalline phases is also an important parameter because osteoblasts prefer a rough surface [37] on which attach and also because coarseness can promote the anchorage of MCM-41 spheres on the scaffolds surface and inside its pores.

Macropores above 100 μm are crucial for the vascularisation of the implant: fig. 7b shows that both for PE1-70 and for PE3-50 the highest contribution to the total area of the pores is given by pores ranging within 100-600 μm. Specifically, about 80% for PE1-70 and almost 90% for PE3-50 of the total pores area consists of pores above 100 μm, and thus large enough to allow blood vessels and cells migration inside the scaffold *in vivo*.

Pores size plays a key role for the colonization of the graft by cells. In fact, it is known that well-engineered scaffolds ought to possess pores sizes and porosities according to the type and the needs of the specific cells that could migrate into the implant. Concerning bone cells, osteoblast size is about 10-50 μm, but pores above 100 μm are necessary to allow the macrophages to enter the implant if, for instance, bacterial infections occur [20]. The proposed scaffolds were also tailored in such a way as to satisfy this requirement.

The presence of micropores (fig. 7a) is also an important feature, because small pores promote cell adhesion and allow the physiological fluids to enter the inner part of the scaffold.

The total porosity, resulting from density measurement, is about 45-50% vol. both for PE1-70 and PE3-50 although a much higher volume amount of polyethylene particles was used for PE1-70 samples preparation. This fact can be explained considering that, in PE1-70 samples, the PE particles size is smaller than in PE3-50 ones: the former scaffolds thus possess a higher number of small pores, involving a greater surface area and reactivity. These features allow a very effective sintering and shrinking of the sample during the thermal treatment resulting in a lower PE%vol./introduced porosity ratio. This feature can also be responsible for the higher mechanical strength observed for series PE1 samples. For all the series of scaffolds, a very low standard deviation in the pore content was observed assessing the reproducibility of the proposed method.

Currently, the prepared scaffolds are under further investigations by means of micro-computed tomography in order to study more accurately the 3-D porous network and the inner structure of the samples.

The amount of total porosity and the densification of sintering necks are the main factors affecting the mechanical properties of the scaffolds. The results of

compressive tests performed on Fa-GC scaffold (PE1-70 and PE3-50) were very satisfactory, because all the samples showed a mechanical strength comparable with the strength of cancellous bone [9]. Besides, the low standard deviation affecting the compressive strength values confirms the good repeatability of the samples.

The composite scaffolds were obtained by soaking both PE1-70 and PE3-50 into the MCM-41 synthesis batch for 12′, so that the silica spheres precipitate inside the pores. XRD analysis performed on MCM-41-PE1-70 scaffold showed a pattern similar to the MCM-41 powder prepared in same conditions (fig. 8). SEM investigations on the composite samples confirmed the presence of MCM-41 spheres, clearly distinguishable and of sub-micronical size, anchored on the pores struts (figures 9, 10 and 11).

The composite scaffolds were tested in compression under the same conditions adopted for PE1-70 and PE3-50 samples. No significant differences, in terms of mechanical strength, were observed among the as-done and composite scaffolds of both the series. This is a very promising result, showing that MCM-41 synthesis batch does not degrade the scaffold structure.

Scaffold pores size affects the distribution of MCM-41 inside the scaffold. In fact, the larger pores of PE3-50 allowed a more effective penetration of MCM-41 spheres (about 2 mm of depth) inside the scaffold, in comparison with PE1-70 (about 1 mm of depth).

The scaffolds showed a bioactive behaviour: HAp agglomerates were observed on the samples surface after 1 week in SBF, as shown in fig. 12. The morphological observations were confirmed by EDS analysis (data not reported) on the agglomerates, which showed the presence of Ca and P in relative amount corresponding to hydroxyapatite. No significant differences were observed

between the MCM-41-loaded scaffolds and the as-done ones, showing that neither MCM-41 synthesis process nor MCM-41 presence inside the scaffold affect its bioactivity.

As far as the drug uptake ability is concerned, MCM-41-PE1-70 can absorb an ibuprofen amount about 10 times greater than PE1-70-ref (table 3), thus assessing that the composite scaffold is a more effective drug carrier. It is worth underlining that the choice of the mesophase is strongly related to the adopted drug molecules (ibuprofen in the present work). In fact, it is crucial to obtain host-guest interactions among the mesophase nanopores and the drug molecules in order to promote a good drug uptake. For this reason, the pores size of prepared MCM-41 spheres (within 1.9-2.0 nm at pH = 9.0 [28]) is comparable to ibuprofen molecule size (length about 1.0 nm).

The release curves, reported in figure 13, are consistent with the results obtained in a previous work for a similar composite system [28]. Moreover, the curves are analogous to those obtained for ibuprofen delivery from MCM-41 powders [36], thus showing that the mesophase plays a key role in ibuprofen release.

5 Conclusions

In this work 3D glass-ceramic scaffold were obtained via uniaxial pressing followed by a thermal treatment in order to remove the organic phase and to sinter the inorganic one. The pores were interconnected and the sintering necks were dense. The obtained scaffolds were covered by HAp agglomerates after 1 week in SBF and possessed a mechanical strength comparable with cancellous bone.

The scaffolds were used as carriers for MCM-41 spheres and then impregnated with ibuprofen, which later on will be delivered by the system. Neither MCM-41

synthesis process nor the presence of MCM-41 spheres, anchored to scaffolds walls, affect the scaffold bioactivity or degrade its structure.

Furthermore, MCM-41-loaded scaffolds can absorb and deliver a greater amount of ibuprofen in comparison with non-loaded ones, assessing the key role played by the mesophase.

Therefore, the prepared Fa-GC scaffolds are good devices for bone substitution and interesting candidates for drug delivery applications.

References

1. J.W. Melvin, Fracture mechanics in bone. J. Biomec. Eng. **115**, 549-554 (1993)
2. W.W. Lu, F. Zhao, K.D.K. Luk, Y.J. Yin, K.M.V. Cheung, G.X. Cheng, K.D. Yao, J.C.Y. Leong, Controllable porosity hydroxyapatite ceramics as spine cage: fabrication and properties evaluation. J. Mater. Sci.: Mater. Med. **14**, 1039-1046 (2003)
3. M. Navarro, S. Del Valle, S. Martinez, S. Zappatelli, L. Ambrosio, J. Planell, New macroporous calcium-phosphate glass-ceramic for guided bone regeneration. Biomaterials **25**, 4233-4241 (2004)
4. E.M. Younger, M.W. Chapman, Morbidity at bone graft donor site. J. Orthop. Trauma **3**, 192-195 (1989)
5. R.G. Boyce, D.M. Toriumi, Considerations in the use of biologic grafts and alloplastic implants in facial plastic and reconstructive surgery. J. Long-Term Effects Med. Implants **2**, 199-220 (1992)
6. M.W. Wolf, S.D. Cook, Use of ostoinductive implants in the treatment of bone defects. Med. Prog. Trough Tecn. **20**, 155-168 (1994)
7. J. Jones, L.L. Hench, Regeneration of trabecular bone using porous ceramics. Curr. Opin. Solid State Mater. Sci. **7**, 301-307 (2003)
8. R.Z. Legeros, S. Lin, R. Rohanizadeh, D. Mijares, J.P. Legeros, Biphasic calcium phosphate bioceramics: preparation, properties and applications. J. Mater. Sci.: Mater. Med. **14**, 201-209 (2003)
9. J.D. Thompson, L.L. Hench LL, Mechanical properties of bioactive glasses, glass-ceramics and composites. J. Eng. in Med. **212**, 127-136 (1998)

10. P.N. De Aza, Z.B. Luklinska, C. Santos, F. Guitian, S. De Aza, Mechanism of bone-like formation on a bioactive implant in vivo. Biomaterials **24**, 1437-1445 (2003)
11. D. Rokusek, C. Davitt, A. Bandyopadhyay, S. Bose, H.L. Hosick, Interaction of human osteoblasts with bioinert and bioactive ceramic substrates. J. Biomed. Res. **75**, 588-594 (2005)
12. M.M. Pereira, A.E. Clark, L.L. Hench, Calcium phosphate formation on sol-gel derived bioactive glasses in vitro. J. Mater. Biomed. Res. **18**, 693-698 (1994)
13. L.L. Hench, Bioactive materials: the potential for tissue regeneration. J. Mater. Biomed. Res. **41**, 511-518 (1998)
14. J.R. Jones, L.M. Ehrenfried, L.L. Hench, Optimising bioactive glass scaffolds for bone tissue engineering. Biomaterials **27**, 964-973 (2006)
15. O. Lyckfeldt, J.M. Ferreira, Processing of porous ceramics by starch consolidation. J. Eur. Ceramic Soc. **18**, 131-140 (1998)
16. N.L. Porter, R.M. Pilliar, M.D. Grynpas, Fabrication of porous calcium polyphosphate implants by solid freeform fabrication: A study of processing parameters and in vitro degradation characteristics. J. Biomed. Mater. Res. **56**, 504-515 (2001)
17. M.H. Prado da Silva, A.F. Lemos, I.R. Gibson, J.M. Ferreira, J.D. Santos, Porous glass reinforced hydroxyapatite materials produced with different organic additives. J. Non-Cryst. Solids **304**, 286-292 (2002)
18. S. Hong Li, J.R. De Wijn, P. Layrolle, K. De Groot, Synthesis of macroporous hydroxyapatite scaffolds for bone tissue engineering. J. Biomed. Mater. Res. **61**, 109-120 (2002)
19. C. Vitale-Brovarone, S. Di Nunzio, O. Bretcanu, E. Verné, Macroporous glass-ceramic materials with bioactive properties. J. Mater. Sci.: Mater. Med. **15**, 209-217 (2004)
20. C. Vitale-Brovarone, E. Verné, L. Robiglio, P. Appendino, F. Bassi, G. Martinasso, G. Muzio, R. Canuto, Development of glass-ceramic scaffolds for bone tissue engineering: Characterisation, proliferation of human osteoblasts and nodule formation. Acta Biomat. **3**, 199-208 (2007)
21. J.E. Babensee, J.M. Anderson, L.V. McIntire, A.G. Mikos, Host response to tissue engineered devices. Adv. Drug. Deliv. Rev. **33**, 111-139 (1998)
22. R. Cancedda, P. Giannoni, M. Mastrogiacomo, A tissue approach to bone repair in large animal models and in clinical practice. Biomaterials **28**, 4240-4250 (2007).
23. P. Horcajada, A. Ramila, K. Boulahya, J. Gonzalez-Calbet, M. Vallet-Regi, Bioactivity in ordered mesoporous materials. Solid State Sci. **6**, 1295-1300 (2004)
24. A. Ramila, B. Munoz, J. Perez-Pariente, M. Vallet-Regí, Mesoporous MCM-41 as drug host system. J Sol-Gel Sci. Tecn. **26**, 1199-1202 (2003)
25. F. Bonneau, L. Yeung, N. Steunou, C. Gervais, A. Ramila, M. Vallet-Regi, Solid state NMR characterization of encapsulated molecules in mesoporous silica. J Sol-Gel Sci. **31**, 219-223 (2004)

26. V. Cauda, S. Fiorilli, B. Onida, E. Verné, C. Vitale-Brovarone, D. Viterbo, G. Croce, M. Milanesio, E. Garrone, Ordered mesoporous silica carried by a bioactive glass-ceramic scaffold for local drug delivery. J. Mater. Sci. :Mater. Med., submitted.
27. C. Vitale-Brovarone, E. Verné, P. Appendino, Macroporous bioactive glass-ceramic scaffolds for tissue engineering. J. Mater. Sci.: Mater. Med. **17**, 1069-1078 (2006)
28. R. Mortera, B. Onida, S. Fiorilli, V. Cauda, C. Vitale-Brovarone, F. Baino, E. Verné, E. Garrone, Synthesis of MCM-41 spheres inside bioactive glass-ceramic scaffold. Chem. Eng. J. **137**, 54-61 (2008)
29. M. Grun, K.K. Unger, A. Matsumoto, K. Tsutsumi, Novel pathways for the preparation of mesoporous MCM-41 materials: control of porosity and morphology. Microp. Mesop. Mater. **27**, 207-216 (1999)
30. D. Ladron de Guevara-Fernadez, C.V. Ragel, M. Vallet-Regi, Bioactive glass-polymer materials for controlled release of ibuprofen. Biomaterials **24**, 2037-2043 (2003)
31. Y.F. Zhu, L. Jian, Y.S. Li, W.H. Shen, X.P. Dong, Storage and release of ibuprofen drug molecules in hollow mesoporous silica spheres with modified pore surface. Microp. Mesop. Mater. **85**, 75-81 (2005)
32. C. Vitale-Brovarone, M. Miola, C. Balagna, E. Verné, 3D-glass-ceramic scaffolds with antibacterial properties for bone grafting. Chem. Eng. J. **137**, 129-136 (2008)
33. T. Kokubo, H. Takadama, How useful is SBF in predicting in vivo bone bioactivity?. Biomaterials **27**, 2907-2915 (2006)
34. F. Di Renzo, A. Galarneau, P. Trens, F. Fajula, in Handbook of Porous Materials, ed. By F. Schuth, K. Sing, J. Weitkamp (Wiley-VCH, 2002), p. 1311
35. P. Horcajada, A. Ramila, J. Perez-Pariente, M. Vallet-Regi, Influence of pore size of MCM-41 matrices on drug delivery rate. Microp. Mesop. Mater. **68**, 105-109 (2004)
36. R. Mortera, S. Fiorilli, E. Garrone, B. Onida, Structural changes of MCM-41 spheres during ibuprofen release to SBF. Stud. Surf. Sci. Catal., **174B**, 1001-1004 (2008).
37. Z. Schwarts, B.D. Boyan, Characterisation of microrough bioactive glasses: surface reactions and osteoblast responses. J. Cell. Biochem. **56**, 340-347 (1994)

Figure

Fig. 1 Trace of Fa-GC DTA

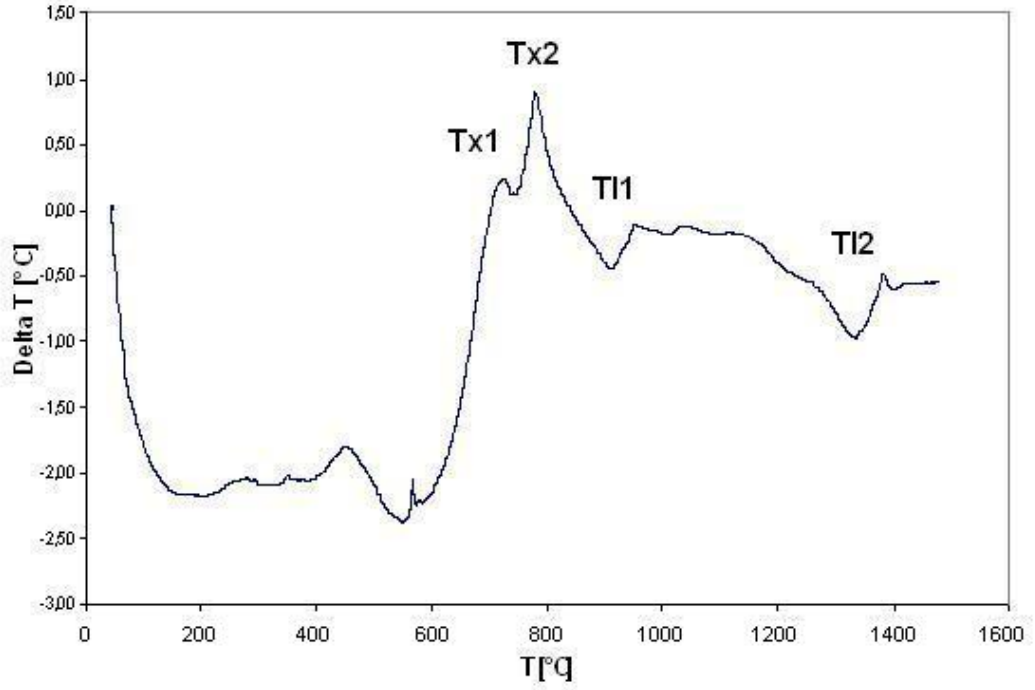

Fig. 2 Diffraction pattern of the as-melt Fa-GC powders (a) and of Fa-GC scaffold (b) (● fluoroapatite peaks, ▲ canasite peaks)

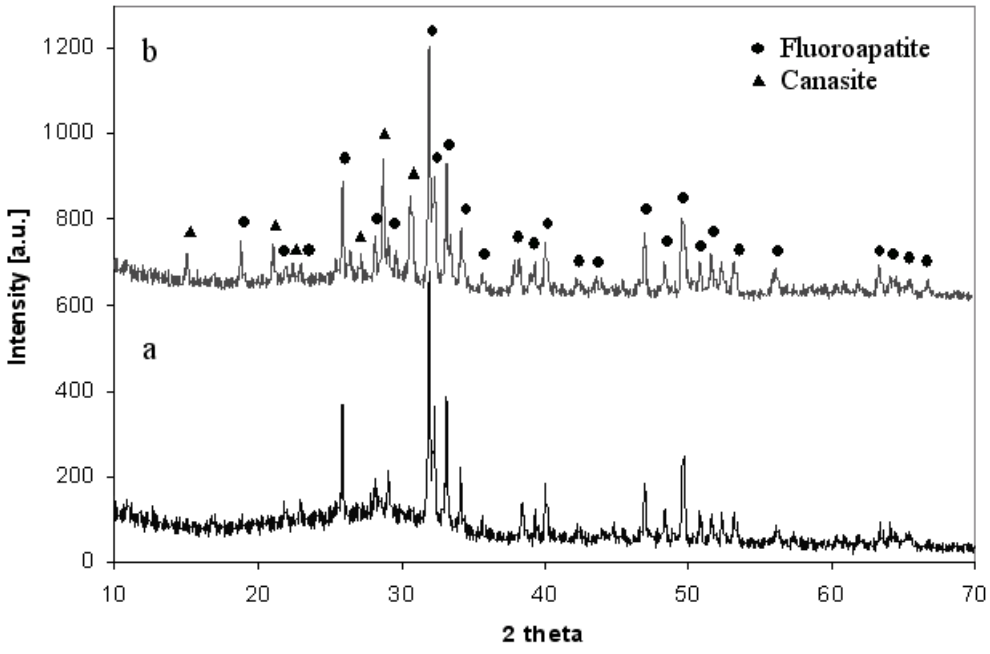

Fig. 3 Variation of Fa-GC sample area during hot stage microscopy

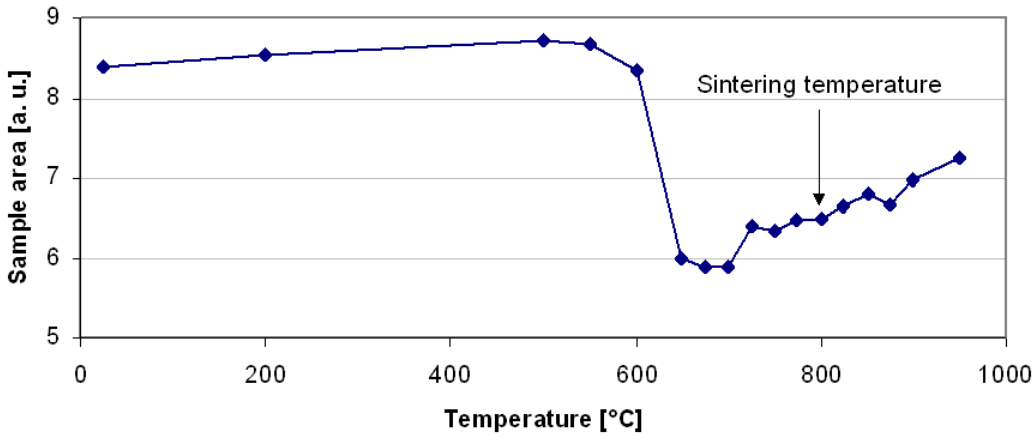

Fig. 4 Micrographs of PE1-40 section (a) and of PE1-70 cross-section (b,c) at different magnifications

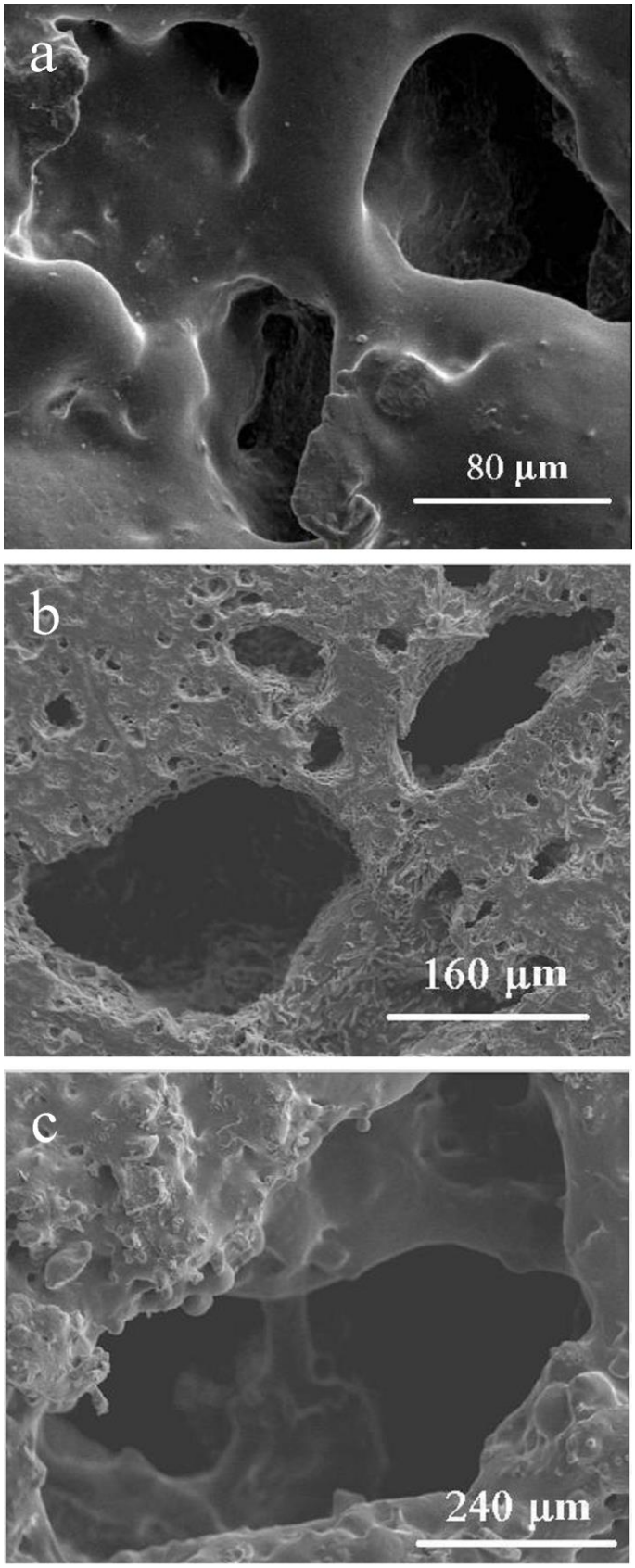

Fig. 5 Micrographs of PE3-50 polished section at different magnifications (a,b) and of a dense sintering neck (c)

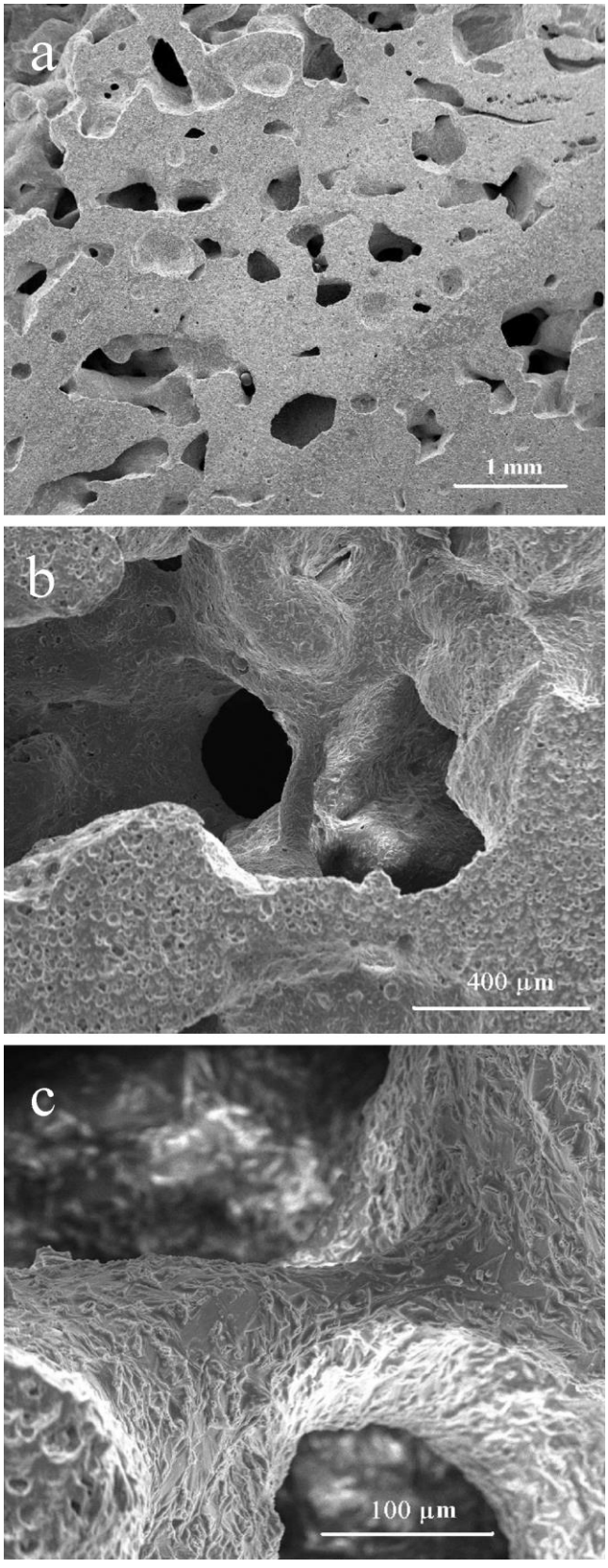

Fig. 6 PE1-70 micrograph for image analysis (a) and PE1-70 processed image (b)

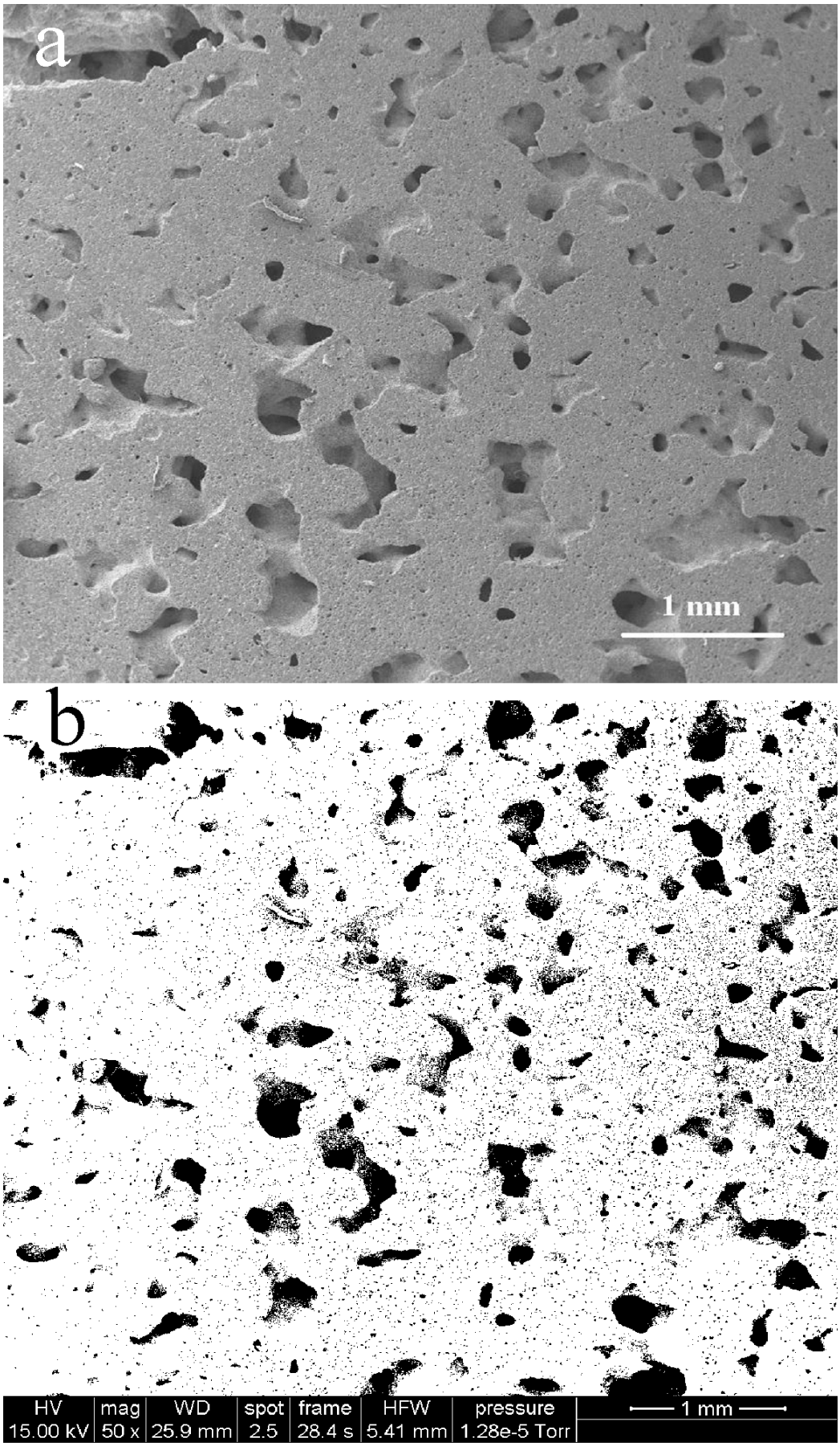

Fig. 7 Comparison of image analysis results for PE1-70 and PE3-50: pores amount (a) and pores area (b)

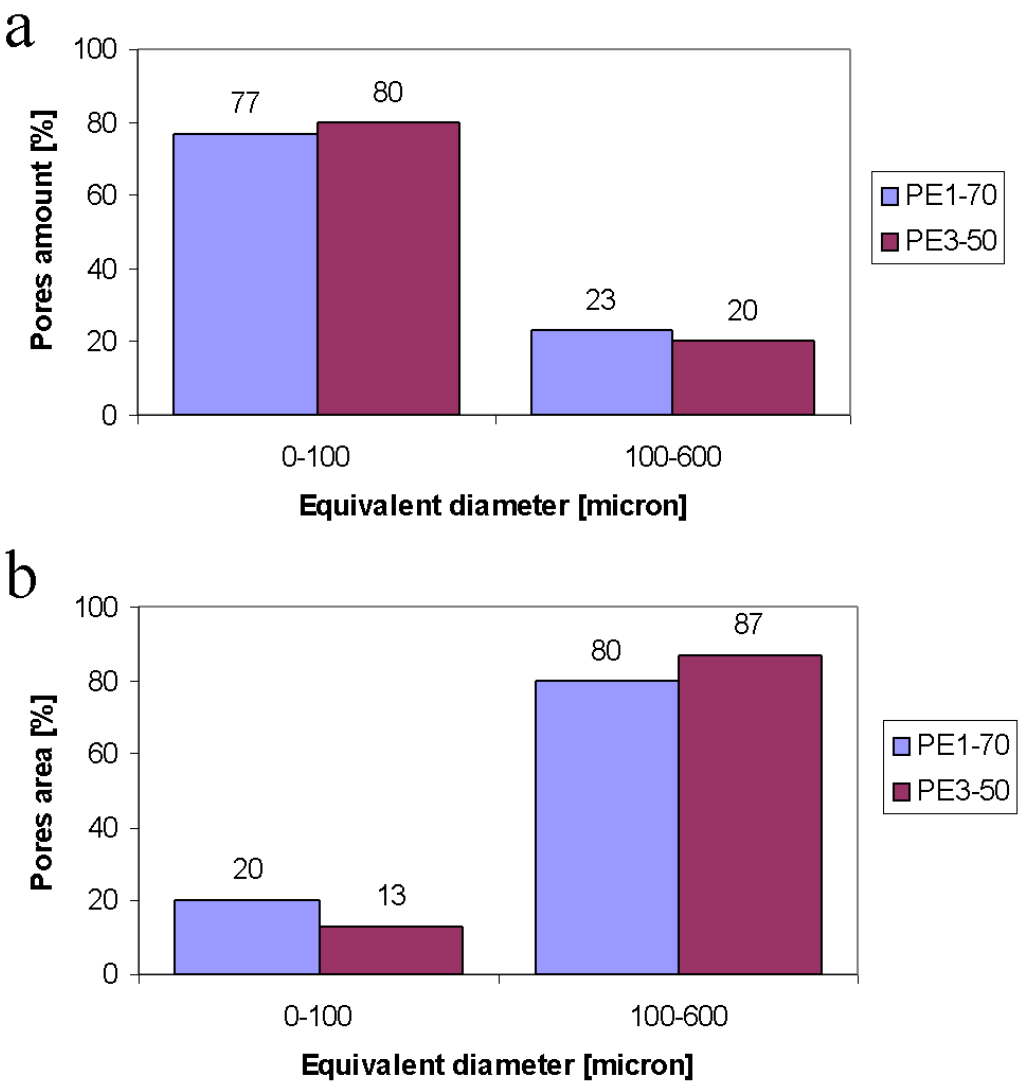

Fig. 8 XRD patterns of MCM41-PE1-70 before (curve 1) and after (curve 2) the calcinations; inset: XRD pattern of calcined MCM-41 in powder (curve A) compared with that of calcined MCM41-PE1-70

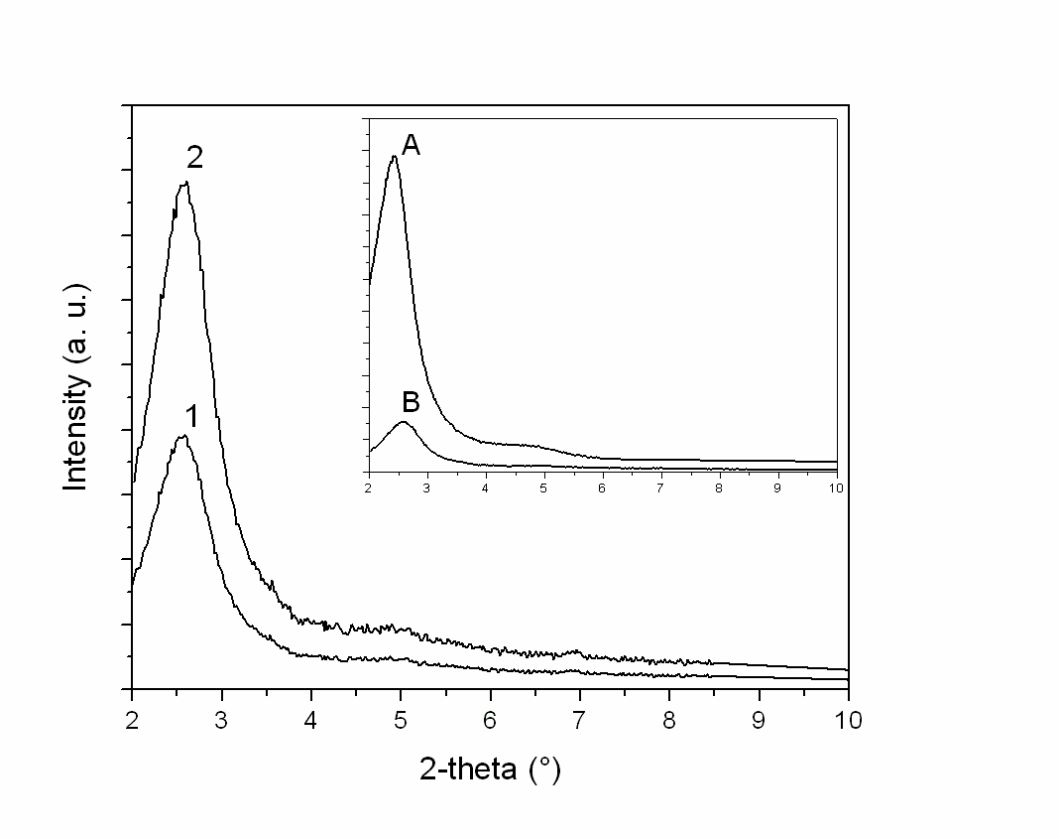

Fig. 9 Micrographs of MCM-41-PE1-70 surface (a) and magnification of a pore (b)

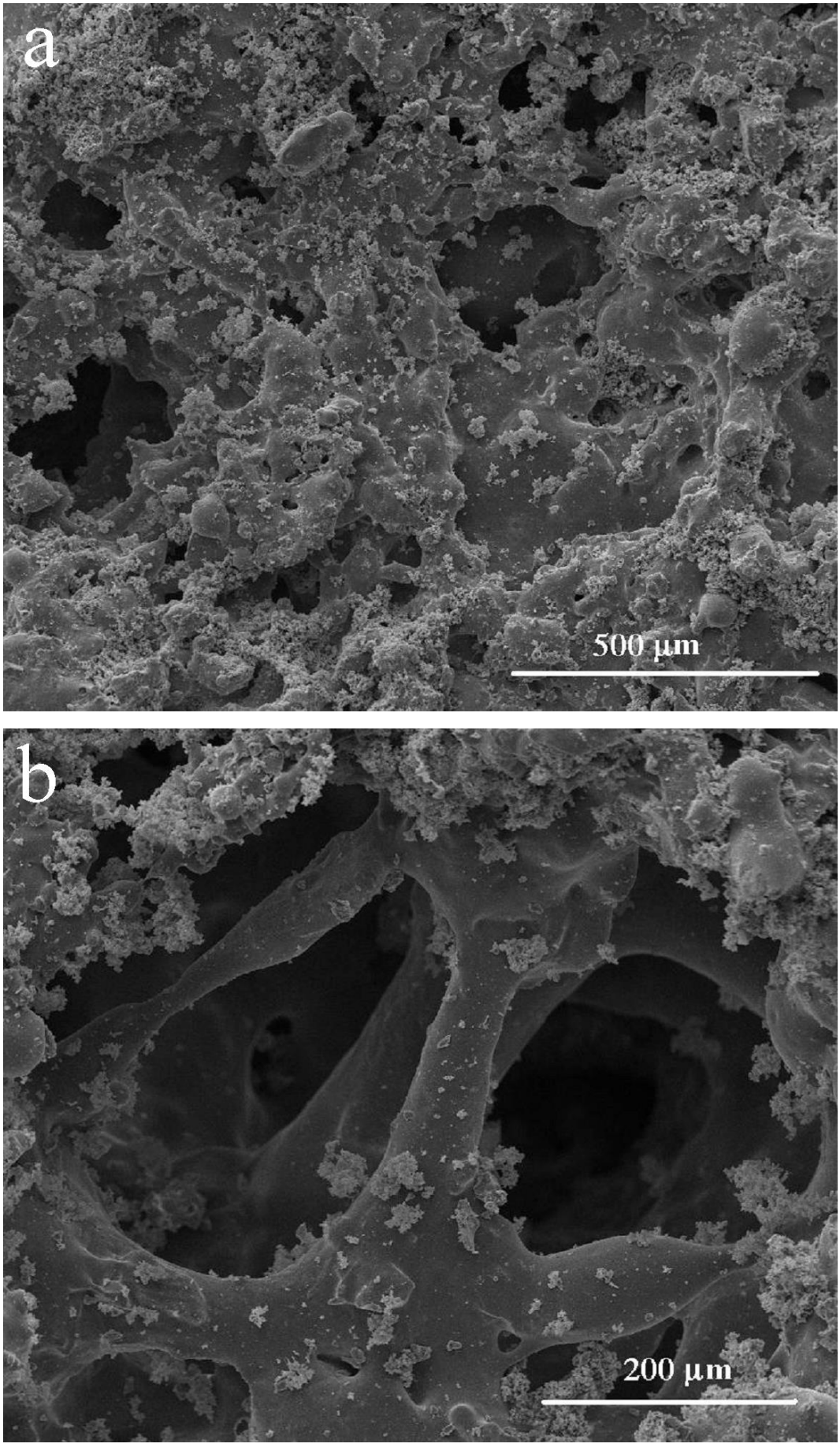

Fig. 10 Micrograph of a double pore on MCM-41-PE1-70 surface (a) and MCM-41 spheres anchored on PE1-70 surface (b)

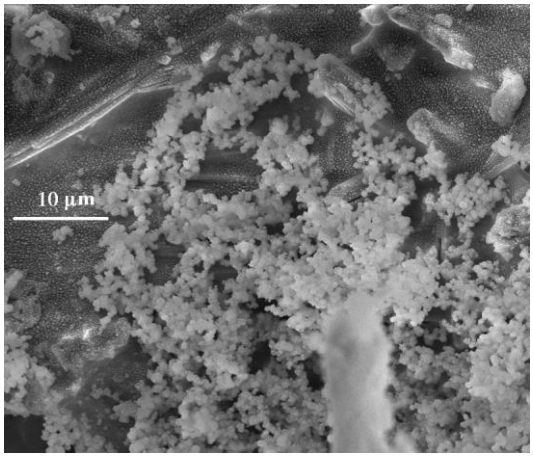

Fig. 11 MCM-41 spheres on PE3-50 surface

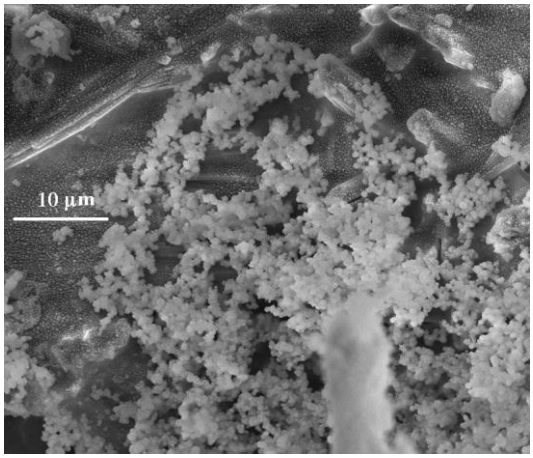

Fig. 12 HAp agglomerate on PE1-70 surface after 1 week in SBF

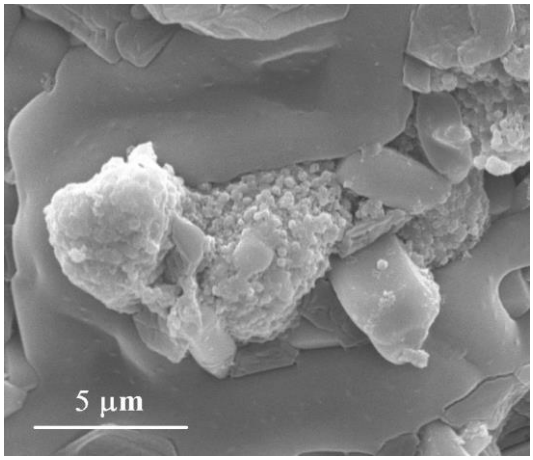

Fig. 13 Release curves in SBF at 37 °C of ibuprofen entrapped in both MCM-41-PE1-70 and PE1-70-ref

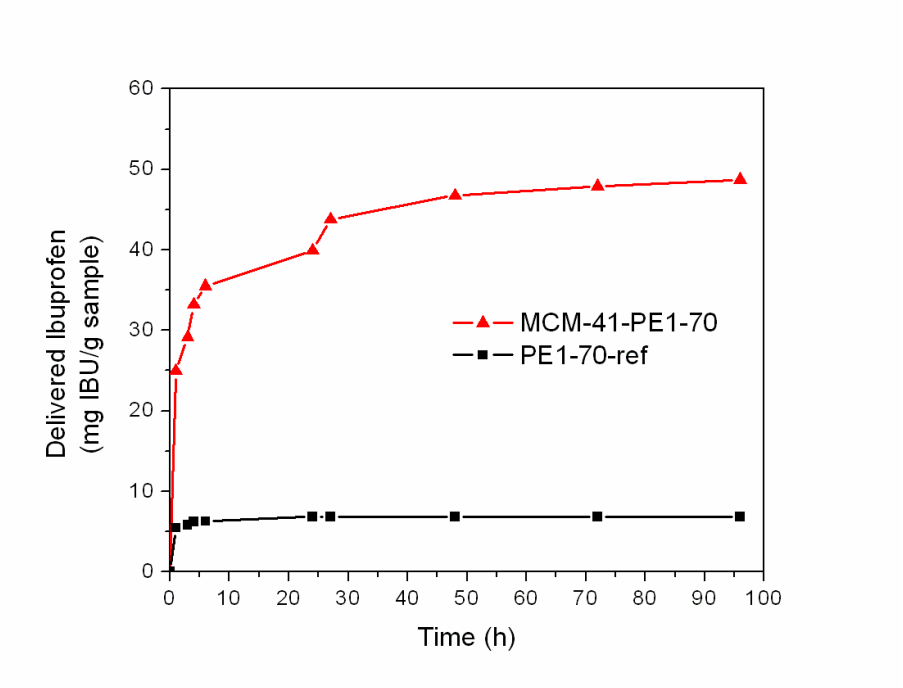

Tables

Table 1 Total porosity obtained via density measurements

Sample	Total porosity (% vol.)
PE1-70	45.0 ± 2.9
PE3-50	51.5 ± 0.7

Table 2 Compressive strength of Fa-GC scaffolds

Sample	Compressive strength [MPa]
PE1-70	21.0 ± 2.9
PE3-50	11.7 ± 2.3

Table 3 Ibuprofen absorbed by the scaffolds

Sample	mg IBU / g scaffold	% weight
PE1-70-ref	7.82	0.78
MCM-41-PE1-70	80.01	8.00